

Dynamics of Land-use/Land-cover and Land Surface Temperature over a period of time in a highly urbanized area using a geospatial approach

Omkar Acharya^{*1}, Dr. Bharat Maitreya²

^{*1}Department of Botany, Bioinformatics and Climate Change Impact Management, School of Science, Gujarat University, Ahmedabad, Gujarat, [*omiacharya@yahoo.com](mailto:omiacharya@yahoo.com)

²Department of Botany, Bioinformatics and Climate Change Impact Management, School of Science, Gujarat University, Ahmedabad, Gujarat, bbmaitreya@gujaratuniversity.in

Abstract: The changes in land use/land cover can potentially impact the land surface temperature. The land-use features that are impenetrable can increase the Land Surface Temperature, while vegetation cover can decrease the Land Surface Temperature. In this study, we examined the Rajkot city in Saurashtra, Gujarat concerning changes in land use and temperature. Here, we used the imageries from Landsat for the years 2000, 2010, and 2020. We also analyzed the Land Surface Temperature to see how the changes in Land Use Land Cover influence the Land Surface Temperature of the city. We found that across three decades, the city's barren land and fallow land have been decreased and settlement, wetlands, vegetation cover, and industrial areas have been increased. Subsequently, the changes in Land Surface Temperature were noticed. The Land Surface Temperature decreased in the regions where barren land and fallow land are decreased while Land Surface Temperature increased in the areas where wetlands and vegetation cover increased. We conclude that the replacement of the barren and fallow land with human settlement and vegetation cover can decrease the Land Surface Temperature at the local scale.

Index Terms: Rajkot, Urbanization, Anthropocene, heat islands, semi-arid

I. INTRODUCTION

The rapid increase in the human population worldwide has led to the exponential growth of the urban built-up areas (Owen et al., 1998). The United Nations has predicted that by the year 2050, 66% of the global population is expected to be lodged in cities. Urbanization is essential in terms of its economic benefits as they

are economically dynamic and provide ease of administrative purposes. Further, the health management and higher education systems are also being improvised in the urban setups, making them crucial for the overall development (Herold et al., 2003). The essential benefits provided by urban landscapes are, specifically in developing countries, are the enhanced opportunities for employment, specialization, and better production of goods and services (Hallegatte and Corfee-Morlot, 2011). However, the urban areas are characterized by the dominance of human built-up, which induces large-scale changes in the land-use/land-cover (LULC) changes, making them the human-modified regions (Liu and Lathrop, 2002). These changes, in turn, induce the negative impacts of rising surface temperatures in the urbanized areas as a result of the loss of natural vegetation with hard land surfaces that do not allow transpiration and evaporation (Kant et al., 2009).

Understanding the interactions between urbanizations and natural processes and anthropogenic LULC changes is crucial for the appropriate and robust land and climate change management (Mantyka-pringle et al., 2012). The rapid urbanization has created multiple issues relating to the environment and socio-economic factors and is collectively known as "LULC change issues" which are increasing at alarming rates (Subasinghe et al., 2016; Roustia et al., 2018; Dissanayake et al., 2019). One such potential LULC Change issue is the increase in the land surface temperature (LST). Several studies have indicated that the urbanized human settlements are comparatively warmer when compared to the non-urban area. The heat-up areas of urbanized setups are known as

* Corresponding Author

urban heat islands, which are rapidly increasing (Babazadeh and Kumar, 2015; Mohan et al., 2012).

The increase in LST at the regional level is triggered by unplanned and unaccounted changes in the LULC. The impenetrable materials that include roads, residential complexes, parking lots, and industrial and commercial areas make the urban setups the principal heat source. Impenetrable materials cause radiation tapping during the daytime, increasing the surface temperature (Staniec et al., 2016). In the nighttime, these surfaces are can potentially cause the re-radiating of the energy which is known as the heat-back phenomenon (Arsiso et al., 2018)

The relationship between the change in LULC and LST, however, defers based on the geographical scale at which the relationship is being investigated. Also, it depends on the climatic zone. For instance, LST increase when the irrigated cropland and forest covers change to built-up areas. In contrast, the LST decreases on the local scale when the areas with the bare soil are transformed into urbanized areas. This is the manifestation of the cooling effect of vegetation through transpiration, shade, and retention of rainwater, whereas urbanized areas can play this role because of the surface and type of material that makes convection more efficient compared to other areas such as bare soil or rocky areas (Rasul et al., 2016).

In this study, we have taken an urban area of Rajkot city to demonstrate how the dynamics in LULC influence the dynamics in LST over three decades. Rasul et al. (2016) suggested that urbanization is developing on the fallow lands and bare soil, it may reduce LST in the semi-arid region. Therefore, we took an example of a semi-arid region and classified the area as per LULC, and investigated how the LST changes with the change in LULC. We hypothesized that urbanization over the bare soil would effectively reduce the LST.

II. METHODOLOGY

A. Study Area

Rajkot city is situated in the southwest region of Gujarat, famously known as Saurashtra (Figure 1). The city is the district headquarter of the Rajkot district and is the largest city in the Saurashtra region and the fourth largest city of the Gujarat state with a total area of 686 km². The city helps boost the region's economy by providing industrial setups for the engineering and auto ancillary industry.

The climate of this region is classified as a hot semi-arid climate (Bush) with hot, dry summers and mild winters as per the Köppen-Geiger climate classification map (Peel et al., 2007). The vegetation of the region is classified into Tropical thorn forests and patches of Dry deciduous forest (Champion & Seth, 1968). Two major water reservoirs i.e. Aji Dam and Lalpari lake are the main source of water for the city and surrounding area.

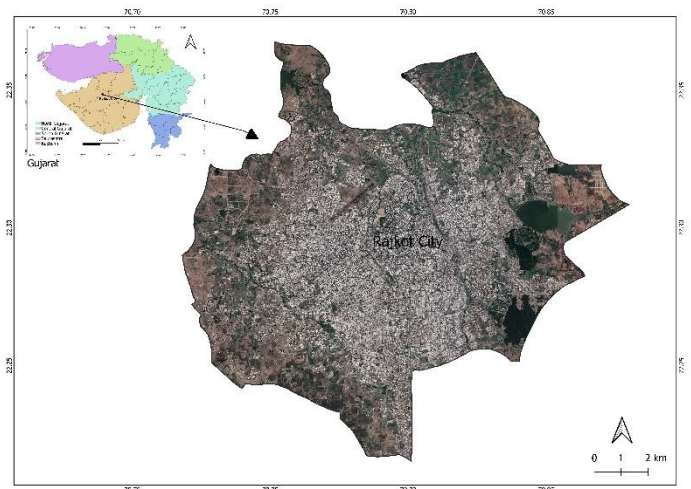


Figure 1. A map showing the Gujarat state and the location of Rajkot city in the Saurashtra region

B. Datasets and Methodology

1) Data Acquisition (Data Sources)

To generate the LULC of the Rajkot city, Landsat 5, 7, and 8 satellite data with a spatial resolution of 30 m were used with a total of six bands that includes Blue, green, Red, and NIR (Near Infrared) & SWIR (Short-wave Infrared 1 & Short-wave Infrared 2). The imageries were downloaded for the months of January-February and a total of three satellite images were utilized.

2) Data Products used (USGS)

The analysis performed on the Level 2 Landsat satellite imagery Products is detailed below in Table 1:

Date of Imagery	Satellite/Sensor	Path/Row
Jan 25, 2000	Landsat- 7/ETM+	150/45
Feb 07, 2010	Landsat-5/TM	150/45
Jan 21, 2020	Landsat-8/OLI	150/45

Table 1. A table showing the details of imageries used in LULC mapping.

The three decadal LULC mappings were performed for the years 2000, 2010, and 2020 using QGIS Software version 3.10 with Semi-Automatic Classification (SCP) Plugin.

3) Image Pre-processing

Landsat Level-2 Pre-processed data was used in the analysis which is also known as surface-reflectance. Layer stacking was carried out in QGIS software using all 6 bands at 30 m resolution, other bands were removed as the resolution of those bands differed from these bands.

Images were clipped by study area shapefile (RMC-Rajkot Municipal Corporation Original Boundary) to set area prefix after noise removal & histogram match. The true-color image was generated and converted to False Color Composite (FCC) for a better understanding of the various land features for Supervised classification.

4) Visual Image Interpretation

To identify objects and judge their significance, a detailed process of image interpretation was undertaken in which the satellite imageries were examined. In this, scrutiny of detection, identification, measurement, and evaluation of environmental and physical objects, patterns, and spatial relationships was done. After the generation of FCC, data was observed by Visual Image interpretation to better understand all features in and around the study area. Majorly shape, color, size, texture, shadow, and pattern was observed for the period of various Land-Use classes.

5) Image Classification

Classification is the process of sorting pixels into a finite number of individual classes, or categories of data based on their data file values. Training class samples made of various reflectance signatures had been generated in ample time before running the supervised classification using the Visual Image Interpretation method on FCCs.

Supervised Classification: Maximum likelihood technique was used for supervised classification for minimum error due to its statistics-based classification which uses a covariance matrix.

Maximum Likelihood Classification calculates the probability that a given pixel belongs to a specific LULC class provided that the normal distribution of the values for each band is followed. Unless you select a probability threshold, all pixels are classified. Map references were collected by NRSC ISRO Map of Gujarat State (WMS) and Bing Map Imagery Base map.

6) Generalized LULC approach

Also, the classified LULC raster was generalized to eliminate the complexity of the information at the pixel level (e.g. removal of pixel noise in an otherwise demarcated area). The Sieve technique was used for this approach.

7) LST computation

To compute Land Surface Temperature, the following steps were followed on the Level-1 data of TIRS i.e. Band 10 in RS-GIS Plugin under QGIS.

- a) *DN (Digital Number) to TOA (Top of the Atmosphere) radiance*

The first step is to convert raw DN into TOA radiance (L_λ) as shown in Eq. 2. This step is necessary to perform as all the pixels will be converted towards the Atmospheric correction of the image.

$$L_\lambda = ML_\lambda \times Q_{cal} + AL_\lambda \quad (2)$$

Where, ML_λ is the radiance multiplicative scaling factor for the respective spectral band, AL_λ is the radiance additive scaling factor for the respective spectral band, and Q_{cal} is the pixel value i.e. DN.

- b) *TOA Radiance to At-satellite brightness temperature (T_λ)*

The next step would render is illustrated by Eq.3.

$$T_\lambda = \frac{K_2}{\ln\left(\frac{K_1}{L_\lambda + 1}\right)} - 273.15 \quad (3)$$

Where L_λ is the radiance, K_1 and K_2 are prelaunch calibration constants (U.S. Geological Survey, 2016). Converting brightness into temperature is as important as getting the accurate pixel resolution towards achieving LST.

- c) *Emissivity calculation before final LST computation*

To compute LST it is required to calculate emissivity (e) as shown in Eq. 4. Emissivity is mentioning the ratio of the energy discharged from a surface at the same temperature and wavelength and under the same observing conditions.

$$e = 0.004Pv + 0.986 \quad (4)$$

Where, Pv is the vegetation proportion and is calculated with the help of scaled Normalized difference vegetation index (by using the NDVI obtained earlier) as shown in Eq. 5.

$$Pv = \left[\frac{NDVI - NDVI_{min}}{NDVI_{max} - NDVI_{min}} \right]^2 \quad (5)$$

Where the NDVI is computed earlier per pixel. While $NDVI_{min}$ and $NDVI_{max}$ are the minima and maximum NDVI respectively. The equation portion in the squared brackets is also called 'scaled NDVI' (Carlson & Ripley, 1997).

- d) *LST Calculation*

Finally, LST is calculated as per Eq. 6.

$$LST = \frac{T_\lambda}{1 + \left(\frac{\lambda \times T_\lambda}{\rho}\right) \ln e} \quad (6)$$

Where, $T\lambda$ is the at-satellite brightness temperature, λ is the wavelength of the emitted radiance, $\rho = h \times c / j$ (h is Planck's constant i.e. $6.62607015 \times 10^{-34}$ Js, c is the velocity of light i.e. 2.99×10^8 m/s and j is the Boltzmann constant i.e. 1.380649×10^{-23} J K⁻¹) and as mentioned earlier the emissivity (ϵ) computed using Eq. 4 will be further used to calculate the final LST (Artis & Carnahan, 1982).

III. RESULTS AND DISCUSSION

A total of three LULC maps of the Rajkot city were generated for the years 2000, 2010, and 2020. Similarly, three more maps were generated of the LST for similar years to compare the changes in both LULC and LST. The accuracy assessment using random point selection revealed the high accuracy (>85%) of all three LULC generated in the study (Table 2).

Year	Overall Accuracy
2000	92.04 %
2010	94.20%
2020	87.72%

Table 2. A table showing the accuracy of LULC mapping

A. Changes in the land cover/land use of the Rajkot city from 2000-to 2020

The LULC classification resulted in a total of seven available land-use types in a landscape that includes: Agriculture, built-up, waterbodies, barren land, fallow land, vegetation patches, and industrial area. The comparison of the percentage contribution of each seven classes across three decades indicated that there is an apparent increase in the area of built-up, water bodies, vegetation patches, and industrial areas. On the other hand, an agricultural area, barren land, and fallow land area decreased over the last three decades (Figure 3).

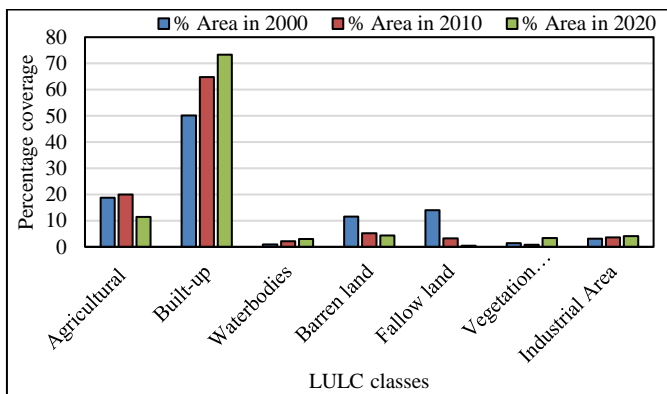


Figure 3. A column graph showing the variation in the percentage area of the seven LULC classes over three decades in and around Rajkot city.

B. Changes in the land surface temperature of the Rajkot city from 2000-to 2020

The spatial analysis of LST showed that there is a linear decrease in the temperature over the last 30 years in Rajkot city. Initially, in 2000, the temperature of the city ranged between 19 to 36 °C. The temperature range narrowed down to 19 to 34 °C in 2010, which again narrowed down to 18 to 31 °C during the year 2020. The results indicated that the variation between the coolest and warmest part of the city is coming closer (Figure 4)

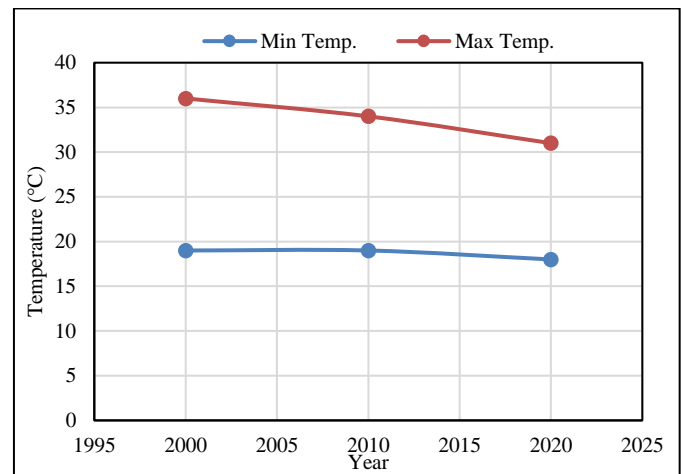


Figure 4. Trend lines of minimum and maximum temperature across three decades in and around Rajkot city.

C. Comparison of variations in the LULC and LST of Rajkot city

1) The year 2000

In Figure 5, it is evident that the LULC and LST of the city are highly correlated. During the year 2000, the southwest parts of the city were dominated by the fallow land and barren land. This is also the same area where the highest LST was recorded for that particular year. This year, fallow land and barren land accounted for 26% of the total area (refer to Figure 3). In correspondence to this, the high-temperature area accounted for more than 60% (visual assessment). It is also evident that the cooler areas in the northern parts are due to the presence of extensive vegetation patches and wetlands in the city.

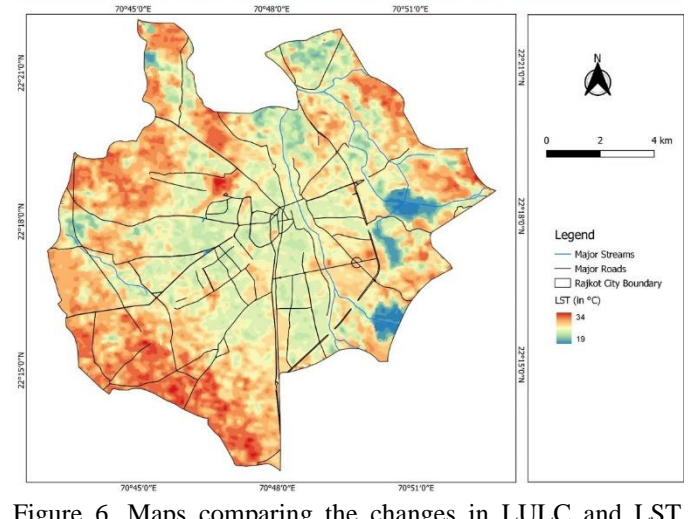
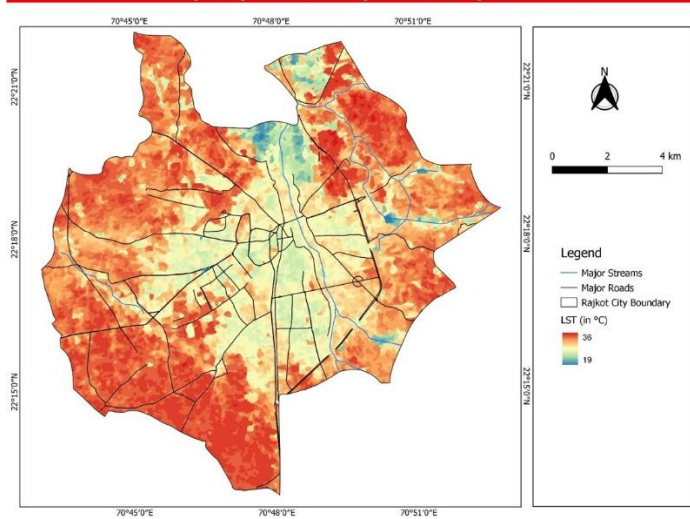
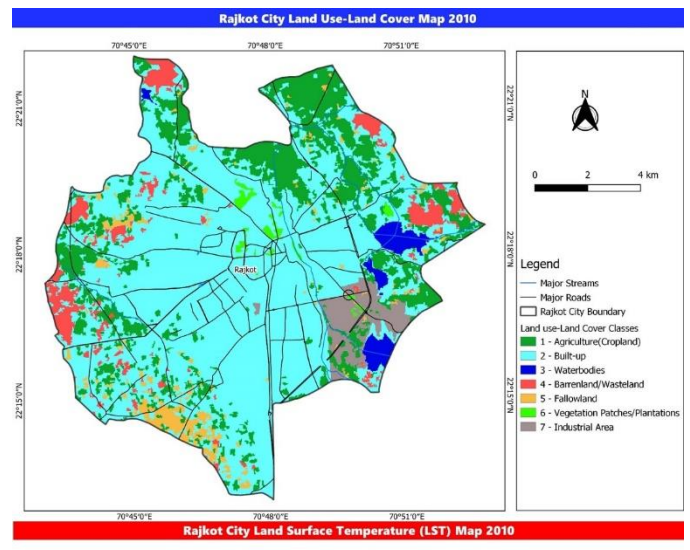
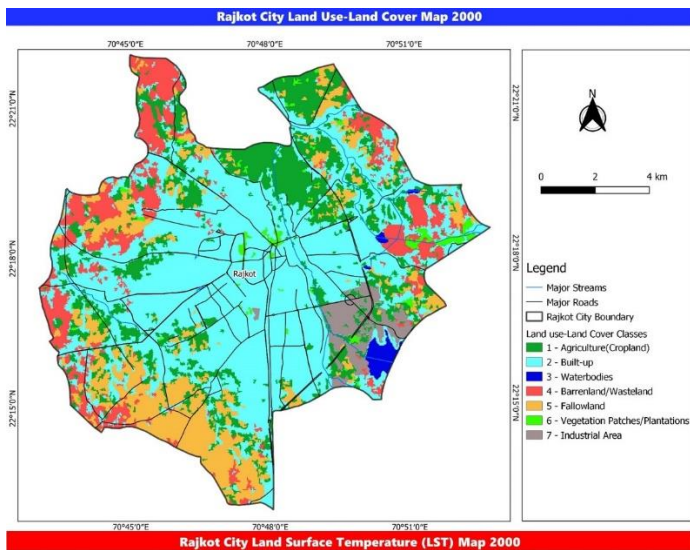


Figure 5. Maps comparing the changes in LULC and LST during the year 2000

Figure 6. Maps comparing the changes in LULC and LST during the year 2010

2) The year 2010

As shown in figure 6, the areas of barren land and fallow land decreased during the year 2010. The percentage contribution of barren land and fallow land decreased to 8% in 2010 from 26 % in 2000. A similar decrease was also observed in the case of high-temperature areas. In the year 2010, visual shrinkage was also observed in high-temperature areas in southwest and northeast parts of the city following the decrease in fallow land-barren land and increase in green patches in the respective regions. Similarly, the temperature decreased in the areas where the waterbody expanse increased.

3) The year 2020

The LULC classification showed a drastic change in the land use of the city when compared to previous years (Figure 7). The built-up area increased significantly and contributed to 73% and barren land and fallow land almost disappeared from the city (5% contribution). When looking at the temperature, the spatial spread of temperature again showed a similar trend to the previous years as the temperature decreased wherever the barren land and fallow land decreased.

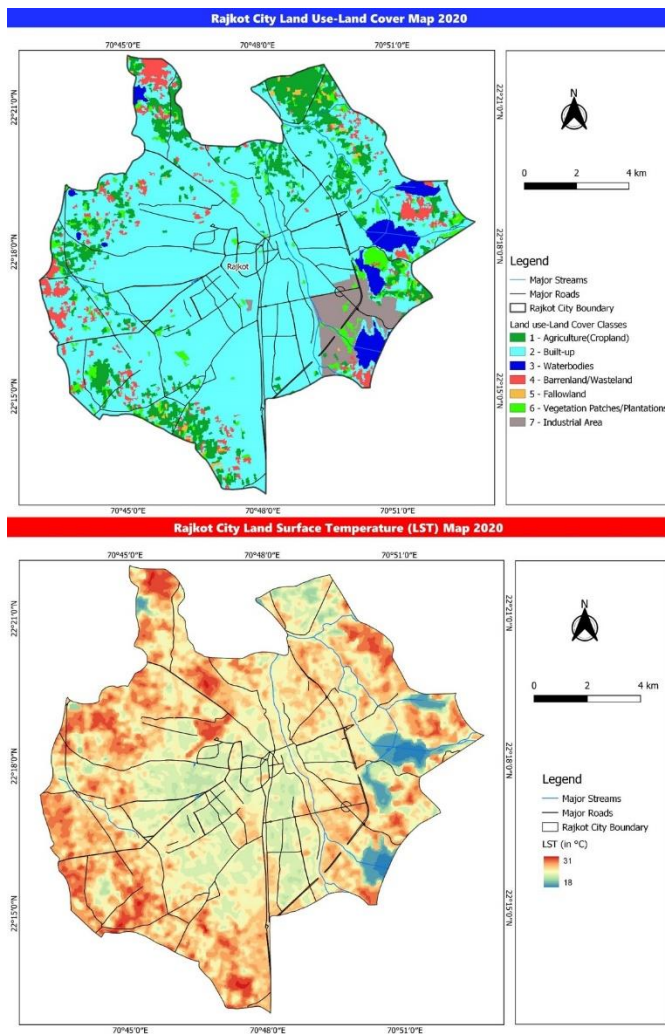


FIGURE 7. MAPS COMPARING THE CHANGES IN LULC AND LST DURING THE YEAR 2020 CONCLUSION

This technical study is revealing the co-relationship between Landuse & Land Surface Temperature. It describes how does satellite data can help to reveal the information about the ground and related changes over the period of 2 decades using various methods and algorithms of Open-source software. As described in the results, The overall decreasing trend was observed in LST in this study. For all the years, it was observed that the temperatures if high in the areas where there is barren land and fallow land available. In contrast, the temperature was observed to be lower in the areas where there was a human settlement. Further, the temperature in industrial setups was lower which was against the general perception that industrial areas generally have high surface temperatures. The finding of this study suggests that the barren land is inducing higher temperatures due to the unavailability of vegetation cover that can provide a cooling effect, as indicated in Rasul et al. (2017). Further, Mehta et al. (2021) suggest that the high NDVI values lower the temperature, which is again confirmed in this study, where the low temperature was recorded in the vegetation patches. In this study, the area with Rajkot city settlement showed constant temperature.

IV. CONCLUSION

The present study has demonstrated that the Land-use/Land-cover can be the surrogate to inform the land surface temperature. However, the imageries used in this study are primarily of ten-year intervals which can be largely improved if the year interval is reduced. Further, the resolution of the Landsat imagery used in this study was 30 m which can be improved by using 10 m imageries. This will provide further insights into the correlation of LULC and LST at a fine scale. Moreover, there is a gradual increase in the built-up area with some fluctuations that can be observed in the dense tree cover and open tree cover. There has also been a gradual decrease in the land area and the water bodies that form the geography of the region. Vegetation indices of about 0.4 to 1, which may be higher than normal were observed in the Northern and Western Rajkot. Low normalized vegetation indices were witnessed in the Southern Easter Areas, with dense urban areas along with some water bodies. There is an increase in the vegetation in the Northern Part of the city with some improvement in the dense vegetation, whereas the North-East part showed some increment in the number of water bodies. Hence, it is observed that there is a good growth in the vegetation to meet the demands of the increasing population. Likewise, there has been an increase in the surface temperature by about 3.7°C from about 41.94°C in the year 2000, to 45.7°C in 2010 which ultimately lead to a hotter Winter Month.

V. REFERENCES

- Arsiso, B.K.; Mengistu Tsidu, G.; Stoffberg, G.H.; Tadesse, T. (2018). Influence of urbanization-driven land use/cover change on climate: The case of Addis Ababa, Ethiopia. *Phys. Chem. Earth* 2018, 105, 212–223.
- Artis, D. A., & Carnahan, W. H. (1982). Survey of emissivity variability in thermography of urban areas. *Remote Sensing of Environment*, 12(4), 313–329. [https://doi.org/10.1016/0034-4257\(82\)90043-8](https://doi.org/10.1016/0034-4257(82)90043-8)
- Babazadeh, M., Kumar, P. (2015). Estimation of the urban heat island in local climate change and vulnerability assessment for air quality in Delhi. *European Scientific Journal* ISSN:1857-7881, 55–65.
- Carlson, T. N., & Ripley, D. A. (1997). On the relation between NDVI, fractional vegetation cover, and leaf area index. *Remote Sensing of Environment*, 62(3), 241–252. [https://doi.org/10.1016/S0034-4257\(97\)00104-1](https://doi.org/10.1016/S0034-4257(97)00104-1)
- Dissanayake, D.; Morimoto, T.; Murayama, Y.; Ranagalage, M. (2019) Impact of landscape structure on the variation of land surface temperature in Sub-Saharan Region: A case study of Addis Ababa using Landsat Data (1986–2016). *Sustainability*, 11, 2257.
- Hallegette, S., & Corfee-Morlot, J. (2011). Understanding climate change impacts, vulnerability, and adaptation at city scale: An introduction. *Climatic Change*, 104(1), 1–12

- Herold, M., Goldstein, N. C., & Clarke, K. C. (2003). The spatiotemporal form of urban growth: Measurement, analysis, and modeling. *Remote Sensing of Environment*, 86(3), 286–302.
- Liu, X., & Lathrop, R., Jr. (2002). Urban change detection is based on an artificial neural network. *International Journal of Remote Sensing*, 23(12), 2513–2518
- Mantyka-pringle, C. S., Martin, T. G., Rhodes, J. R., (2012). Interactions between climate and habitat loss effects on biodiversity: a systematic review and meta-analysis. *Glob. Change Biol.* 18, doi:10.1111/j.1365–2486.2011.02593.x.
- Mohan, M., Kikegawa, Y., Gurjar, B. R., Bhati, S., Kandya, A., Ogawa, K. (2012). Urban heat island assessment for a tropical urban airshed in India. *Journal of Atmospheric and Climate Sciences* 2, 127–138.
- Owen, T., Carlson, T., & Gillies, R. (1998). An assessment of satellite remotely-sensed land cover parameters in quantitatively describing the climatic effect of urbanization. *International Journal of Remote Sensing*, 19(9), 1663–1681
- Peel, M. C., Finlayson, B. L., & McMahon, T. A. (2007). Updated world map of the Köppen-Geiger climate classification. *Hydrology and Earth System Sciences*, 11(5), 1633–1644. <https://doi.org/10.5194/hess-11-1633-2007>
- Rajkot District Collectorate, Rajkot CDP 2005-2012
- Rajkot District Collectorate, Socio-Economic Profile 2006-07, Gujarat Seismic Zone Map
- Rasul, A., Balzter, H., & Smith, C. (2016). Diurnal and seasonal variation of surface Urban Cool and Heat Islands in the semi-arid city of Erbil, Iraq. *Climate*, 4(3). <https://doi.org/10.3390/cli4030042>
- Rousta, I.; Sarif, M.O.; Gupta, R.D.; Olafsson, H.; Ranagalage, M.; Murayama, Y.; Zhang, H.; Mushore, T.D. (2018). Spatiotemporal analysis of land use/land cover and its effects on surface urban heat Island using Landsat data: A case study of Metropolitan City Tehran (1988–2018). *Sustainability*, 10, 4433
- Staniec, M.; Nowak, H. (2016). The application of energy balance at the bare soil surface to predict annual soil temperature distribution. *Energy Build.*, 127, 56–65.
- Subasinghe, S.; Estoque, R.C.; Murayama, Y. (2016) Spatiotemporal analysis of urban growth using GIS and remote sensing: A case study of the Colombo Metropolitan Area, Sri Lanka. *ISPRS Int. J. Geo Inf.*, 5, 197.
- U.S. Geological Survey. (2016). Landsat 8 Data Users Handbook. *Nasa*, 8(June), 97. <https://landsat.usgs.gov/documents/Landsat8DataUsersHandbook.pdf>
- United Nations. UN Department of Economic and Social Affairs, *World Urbanization Prospects: The 2014 Revision, Highlights*; United Nations: New York, NY, USA, 2015
- Mitesh Gohil; Ravi Dutt Kamboj; Dr. Rajkumar S Yadav; *Investigating and Analysis of Land Use/ Land Cover (LULC) change using remote sensing image interpretation for the urban area of Rajkot Municipal Corporation, Gujarat* (2021) ; *Disaster Advances*, 14, 28, 34
- Madhuri K.; Nishant J.; *Spatiotemporal Analysis of Urban Growth, Sprawl and Structure of Rajkot, Vadodara, and Surat (Gujarat-India) based on Geographic Information Systems, in Relation to the Sustainability Pentagon Analysis* (October-2015); *Indian Journal of Science and Technology*, Vol 8(28) ISSN: 0974-6846, 0974-5645
- Vose, R. S., T. R. Karl, D. R. Easterling, C. N. Williams, and M. J. Menne, 2004: *Impact of land-use change on climate. Nature*, 427, 213–214.
- Steyaert, L. T., and R. G. Knox, 2008: *Reconstructed historical land cover and biophysical parameters for studies of land-atmosphere interactions within the the eastern United States. J. Geophys. Res.*, 113, D02101, doi:10.1029/2006JD008277.
- K. Tarun and D. C. Jhariya "Land quality index assessment for agricultural purpose using multi-criteria decision analysis (MCDA)", *Geocarto International*, 822-841, 2015.
- C. K. Singh, S. Shashtri, S. Mukherjee, R. Kumari, R. Avatar, A. Singh, R. P. Singh "Application of GWQI to Assess Effect of Land Use Change on Groundwater Quality in Lower Shiwaliks of Punjab: Remote Sensing and GIS-Based Approach", *Water Resources Management*, 25:1881–1898, 2011.
- N.C. Anil, G.J. Sankar, M. J. Rao, I.V.R.K.V. Prasad and U. Sailaja Studies on Land Use/Land Cover and change detection from parts of South West Godavari District, A.P – Using Remote Sensing and GIS Techniques. *J. Ind. Geophys. Union* Vol.15, No.4, pp.187-194, October 2011
- Agarwal, C., G. M. Green, J. M. Grove, T. P. Evans, and C. M. Schweik. 2002. *A Review and Assessment of Land-Use Change Models: Dynamics of Space, Time, and Human Choice*. General Technical Report NE-297. Newtown Square, Pennsylvania: U.S. Department of Agriculture, Forest Service, Northeastern Research Station. 61 pp.
- Wackernagel M., Schulz N.B., Deumling D, Linares A.C., Jenkins M., Kapos V., Monfreda C., Loh J., Myers N., Norgaard R., and Randers J. 2002. Tracking the ecological overshoot of the human economy *Proceedings of National Academy of Sciences USA*, 99(14). 9266–9271.
